 CMES, vol.33, no.3, pp.243-267, 2008

Node based Method of Moments Solution to Combined Layer Formulation of Acoustic Scattering

B. Chandrasekhar[1]

Abstract: In this work, a novel numerical technique, based on method of moments solution, is presented to solve the Combined layer formulation (CLF) to insure unique solution to the exterior acoustic scattering problem at all frequencies. A new set of basis functions, namely, Node based basis functions are used to represent the source distribution on the surface of rigid body and the same functions are used as testing functions as well. Combined layer formulation (CLF) is defined by linearly combining the Single layer formulation (SLF) and Double layer formulation (DLF) with complex coupling parameter. The matrix equations for the SLF and DLF are derived and same equations are extended to the CLF. The surface of the body is modeled by triangular patch modeling. Results of numerical technique presented in this paper, using node based basis functions, are compared with the exact solutions wherever available. Also, condition numbers of the impedance matrices of SLF, DLF and CLF are plotted, for some objects of canonical shapes, to show that only CLF is free from resonance problem.

Keyword: Acoustic scattering, Method of moments, Node based basis function, Boundary integral equations, Acoustic resonance problem, Non-uniqueness.

1 Introduction

The non-uniqueness of the solution of exterior acoustic problems is widely discussed in the recent literature and has been one of the interesting areas of research for long time. Non-uniqueness of solution is the breakdown of the formulations when the frequency of incident acoustic wave matches with the eigen-frequencies of the corresponding interior problem. Though exterior acoustic scattering problems do not have any characteristic frequencies associated with it, the integral equations do fail at certain frequencies due to the boundary integral equation formulation. More details regarding the fictitious frequencies can be found in the

[1] Supercomputer Education and Research Center, Indian Institute of Science, Bangalore. India-560012.

ref. [Chen and Chen (2006), Chen, Chen and Chen (2006)]. The adjoint of these boundary integral equations represent the interior acoustic problems which has got well known characteristic frequencies. Hence boundary integral equations for the exterior acoustic problems fail when the incident wave frequency matches with the characteristic frequencies of the surface bounding the scattering volume. Two popularly known methods to resolve the non-uniqueness problem in the exterior acoustic problems are 1. Combined Helmholtz Integral Equation Formulation (CHIEF) and 2. Burton and Miller's approach.

CHIEF, proposed by Schenck [Schenck (1968)] is very popular among various engineering applications. CHIEF is basically addition of some interior relations to the surface Helmholtz integral equation thus resulting in a over determined system of equations. This over determined system of equations may be solved by the least squares technique. One of the major drawbacks of this formulation is the selection of CHIEF points to insure a uniqueness of the solution. A "good" CHIEF point to be chosen in such a way that it should be away from the neighborhood of nodal point of the corresponding interior eigenmode. Although CHIEF is very popular, it is heuristic and prone to inaccuracies especially at higher frequencies.

Another popular method of resolving the non-uniqueness issue is Burton and Miller's (BM) approach. BM approach [Burton and Miller (1971)] basically suggests linearly combining the Helmholtz integral equation and its normal derivative with a complex coupling parameter. Leis [Leis (1965)], Panich [Panich (1965)], and, Brakhage and Werner [Brakhage and Werner (1965)] also demonstrated that by combining the single layer and double layer potentials with a complex coupling parameter, the non-uniqueness problem can be averted. Burton and Miller proved mathematically that, this linearly combined integral equation insures unique solution at all frequencies. But, the normal derivative of the Helmholtz integral equation involves the evaluation of hyper-singular integral. Many researchers [Amini and Wilton (1986), Meyer, Bell, Zinn, and Stallybras (1978), Chien, Raliyah and Alturi (1990), Yan, Cui and Hung (2005)] attempted to evaluate the hyper-singular integral which may be used in the BM procedure to overcome the internal resonance problem. The usual procedure is to regularize the hyper–singular integral and the regularization technique is computationally very expensive and it is difficult to incorporate in a general-purpose code. Also, there are other methods which reduce the hyper singular kernel to a strongly singular kernel and their solution is based on Petrov-Galerkin schemes [Qian, Han, and Atluri (2004)] and collocation-based boundary element method [Qian, Han, Ufimtsev, and Atluri (2004)]. A desingularized boundary integral formulation is also one of the recently proposed method [Callsen, von Estorff, and Zaleski (2004)] to overcome the problems of singularity.

Recently, Chandrasekhar and Rao [Chandrasekhar and Rao (2004b)] extended concept of BM approach by linearly combining the integral equations based on layer potentials in contrast to combining the Helmholtz integral equation and its normal derivative as suggested by Burton and Miller. They adapted the method of moments solution as a numerical technique to implement the combined layer formulation (CLF). The procedure [Chandrasekhar and Rao (2004a)] that they followed neither regularizes the hyper-singular integral nor implements complex integration schemes. They also extended the same numerical procedure to the acoustic scattering from open bodies and intersecting bodies [Chandrasekhar and Rao (2005)]. The method of moments solution that they proposed was based on defining the basis functions on the edges of the triangular patch modeling of the surface of the scattering body. As the method of moments solution results in a full matrix, the size of the resulting impedance matrix, based on defining the basis functions on the edges, is large. Recently, author [Chandrasekhar (2005)] has implemented the method of moments solution of single layer and double layer formulations based on defining the basis functions on the nodes in contrast to defining it on the edges. For a closed body, the relationship between the number of nodes N_n, edges N_e and patches N_f in the triangular patch modeling is given by $N_n - N_e + N_f = 2$ and $N_f = 2N_e/3$ [Oneill]; this results into $N_n = 2 + N_e/3$. Thus the order of the resulting matrix, defining the basis functions on the nodes, is almost one third to that of defining the basis functions on edges. As the storage matrix is smaller, time required for the solution of simultaneous linear system of equations is smaller and hence, much larger problems can be solved without increasing the solution time compared to the existing solutions based on method of moments with face based basis functions [Raju, Rao, Sun (1991), Rao and Sridhara (1991), Rao, Raju, and Sun (1992), Rao and Raju, (1989)] and with edge based basis functions [Chandrasekhar and Rao (2004a)].

In this work, the non-uniqueness problem is eliminated by implementing the combined layer formulation (CLF) using method of moments solution procedure with node based basis functions. Traditionally, DLF is difficult to implement due to the presence of hyper-singular kernel. In this work simple vector calculus techniques are used to circumvent the problems of hyper-singularity.

The method developed in this work can be used in combination with other methods like Mesh Less Petrov-Galerkin schemes [Vavourakis, Sellountos and Polyzos (2006); Sladek, Sladek, Wen and Aliabadi (2006); Gao, Liu and Liu (2006); Zhang and Chen (2008); Sladek, Sladek, Solek and Wen (2008); Dang and Bhavani Sankar (2008); and Arefmanesh, Najafi and Abdi, (2008)] and boundary element formulations, but not limited to acoustic scattering [Owatsiriwong, Phansri, and Park (2008); Criado, Ortiz, Manti c, Gray, and Paris (2007); Chandrasekhar and Rao.

(2007); Zai You Yan (2006); and Soares Jr, and Vinagre (2008)].

2 Organization of the paper

In this paper, next section briefly describes the method of moment's solution procedure [Harrington (1968), Sun and Rao(1992)]. Mathematical formulation is laid in section 4 for SLF, DLF and CLF. In section 5, we describe the numerical solution procedure and derive matrix equations for SLF, DLF and CLF. Numerical results, based on the development of new basis functions are given in section 6. Lastly we present some important conclusions drawn from the present work.

3 Outline of Method of Moments

Consider the deterministic equation

$$Lf = g \tag{1}$$

where L is a linear operator, g is a known function and f is an unknown function to be determined. Let f be represented by a set of known functions f_j, $j = 1,2,...,N$ termed as basis functions in the domain of L as a linear combination, given by

$$f = \sum_{n=1}^{N} \beta_j f_j \tag{2}$$

where β_j are scalar coefficients to be determined. Substituting Eq. 2 into Eq. 1, and using the linearity of L, we have

$$\sum_{n=1}^{N} \beta_j L f_j = g \tag{3}$$

where the equality is usually approximate. Let $(w_1, w_2, w_3, ...)$ define a set of testing functions in the range of L. Now, taking the inner product of Eq. 3 with each w_i and using the linearity of inner product defined as $\langle f, g \rangle = \int_s f \bullet g ds$, we obtain a set of linear equations, given by

$$\sum_{n=1}^{N} \beta_j \left\langle w_i, L f_j \right\rangle = \langle w_i, g \rangle \quad i = 1,2,...,N. \tag{4}$$

The set of equations in Eq. 4 may be written in the matrix form as

$$ZX = Y \tag{5}$$

which can be solved for X using any standard linear equation solution methodologies. The simplicity, accuracy and efficiency of the method of moments lies in choosing proper set of basis/testing functions and applying to the problem at hand. In this work, we propose a special set of basis functions and a novel testing scheme to obtain accurate results using SLF, DLF and CLF.

4 Mathematical Formulation

Consider an acoustic wave, with a pressure and velocity $\left(p^i, u^i\right)$, incident on a three-dimensional arbitrarily shaped rigid body placed in a source free homogeneous medium of density ρ and speed of sound c through the medium. When the incident wave interacts with the body, the acoustic wave gets scattered with a pressure and velocity (p^s, u^s). Here, we note that, incident fields are defined in the absence of the scattering body. Φ is the scalar velocity potential satisfying the Helmholtz differential equation $\nabla^2\Phi + k^2\Phi = 0$ for the time harmonic waves present in the region exterior to the surface S of the body. One more condition on velocity potential is that it should satisfy the appropriate boundary conditions on the surface S of the body along with the Sommerfeld radiation condition. The pressure and velocity fields of acoustic wave is related to the scalar velocity potential Φ as $u = -\nabla\Phi$ and $p = j\omega\rho\Phi$. In this paper, integral equation formulations are based on potential theory and free space Green's function. The scattered velocity potential may be defined using three different formulations based on monopole and/or dipole distribution. Formulations based on monopole distribution and dipole distribution are called as single layer formulation (SLF), double layer formulations (DLF), respectively. Third formulation, namely Combined layer formulation (CLF) is a linear combination of SLF and DLF.

Using the potential theory and the free space Green' s function, the scattered velocity potential Φ^s may be defined as

$$\Phi^s = \int_s \sigma\left(r'\right) G\left(r, r'\right) ds' \tag{6}$$

for SLF,

$$\Phi^s = \int_s \sigma\left(r'\right) \frac{\partial G\left(r, r'\right)}{\partial n'} ds' \tag{7}$$

for DLF, and

$$\Phi^s = \int_s \sigma\left(r'\right) G\left(r, r'\right) ds' + \alpha \int_s \sigma\left(r'\right) \frac{\partial G\left(r, r'\right)}{\partial n'} ds' \tag{8}$$

for CLF.

In the above three equations, σ is the source density function independent of r over the surface of the body, r and r' are the position vectors of observation and source points, respectively, with respect to a global co-ordinate system O, and $\partial G/\partial n'$ is the normal derivative of Green's function at source point. Coefficient α is a complex coupling parameter, to be chosen based on the guidelines given by Burton and Miller [Burton and Miller (1971)].

$$k \text{ real or imaginary } \Rightarrow \mathrm{Im}(\alpha) \neq 0 \tag{9}$$

$$k \text{ complex } \Rightarrow \mathrm{Im}(\alpha) = 0 \tag{10}$$

where k is the wave number in the medium.

$G(r,r')$ is the free space Green's function, given by,

$$G\left(r,r'\right) = \frac{e^{-jk|r-r'|}}{4\pi\left|r-r'\right|} \tag{11}$$

$G(r,r')$ is the solution of the Helmholtz equation with a point source inhomogeneity

$$\left(\nabla^2 + k^2\right) G(r,r') = -\delta\left(r-r'\right) \tag{12}$$

and can be interpreted as the solution at the observation point r due to the presence of acoustic source of unit strength located at the source point r'.

For a rigid body, the normal derivative of total velocity potential, which is the sum of incident and scattered velocity potential, with respect to the observation point on the surface of the body vanishes. That is

$$\frac{\partial\left(\Phi^i + \Phi^s\right)}{\partial n} = 0 \tag{13}$$

$$\frac{\partial \Phi^s}{\partial n} = -\frac{\partial \Phi^i}{\partial n}. \tag{14}$$

Substituting Eqs. 6, 7 and 8. into Eq. 14,

$$\frac{\partial}{\partial n}\int_s \sigma\left(r'\right) G\left(r,r'\right) ds' = -\frac{\partial \Phi^i}{\partial n} \tag{15}$$

for SLF,

$$\frac{\partial}{\partial n}\int_s \sigma\left(r'\right) \frac{\partial G(r,r')}{\partial n'} ds' = -\frac{\partial \Phi^i}{\partial n} \tag{16}$$

for DLF, and

$$\frac{\partial}{\partial n}\int_s \sigma\left(r'\right) G\left(r,r'\right) ds' + \alpha\frac{\partial}{\partial n}\int_s \sigma\left(r'\right) \frac{\partial G(r,r')}{\partial n'} ds' = -\frac{\partial \Phi^i}{\partial n} \tag{17}$$

for CLF.

In the above equations, Φ^i is the scalar velocity potential of the incident wave.

Eq. 15, the SLF can also be re-written as

$$\frac{\sigma(r')}{2} - \int_s \sigma(r') \frac{\partial G(r,r')}{\partial n} ds' = \frac{\partial \Phi^i}{\partial n}. \tag{18}$$

The second term in the above equation is the integration over the surface excluding the principal value term i.e. $r = r'$. We note that, this integral is a well behaved integral, although rapidly varying, which can be evaluated using standard integration algorithms.

Following the procedures developed in [Maue (1949) and Mitzner (1966)], Eq. 16, the DLF, may be written as

$$\int_s n \bullet n' k^2 \sigma(r') G(r,r') ds' + \int_s \left(n' X \nabla' \sigma\right) \bullet (nX\nabla G)\, ds' = \frac{\partial \Phi^i}{\partial n} \tag{19}$$

where n and n' are the unit normal vectors at r and r', respectively.

From Eq. 18 and Eq. 19, the CLF can be written as

$$\frac{\sigma(r')}{2} - \int_s \sigma(r') \frac{\partial G(r,r')}{\partial n} ds' + \alpha \int_s n \bullet n' k^2 \sigma(r') G(r,r') ds' + \alpha \int_s \left(n' X \nabla' \sigma\right) \bullet (nX\nabla G)\, ds' = \frac{\partial \Phi^i}{\partial n}. \tag{20}$$

In the following sections, a novel numerical technique is developed using node based basis functions for SLF, DLF and CLF. SLF and DLF fail when the frequency of the incident field matches with the characteristic frequency of surface S. Burton and Miller [Burton and Miller (1971)] suggested combining the Helmholtz integral equation and its normal derivative linearly with a complex coupling parameter to eliminate the internal resonance problem. However, the same concept is extended in this paper to combine the single and double layer formulations with a complex coupling parameter and hence the name Combined layer formulation (CLF). CLF do not fail at the characteristic frequencies and ensures a unique solution at all incident frequencies.

This paper focuses on the numerical solution of single layer, double layer and combined layer formulations by using a new set of basis functions, namely, node based basis functions. The numerical solution of SLF and DLF is already reported in [Chandrasekhar (2005)] and it is the endeavor of this paper to extend the numerical solution to CLF as well to get the unique solution to the acoustic scattering

problems based on the integral equation formulation. As the CLF is a linear combination of SLF and DLF, the matrix equations for SLF and DLF are also derived in this paper.

5 Numerical Solution Procedure

Fig.1 shows the triangular patch modeling of the surface of a arbitrarily shaped three dimensional body. The triangular patch modeling is an approximation of the surfaces. The accuracy of approximation can be increased by modeling the surface with large number of triangular patches of smaller size. The three geometric entities that are present in the triangular patch modeling are triangular patches, edges and nodes. Let N_f, N_e and N_n represent the number of triangular patches, number of edges and number of nodes, respectively, on the surface of triangulated body. For a closed body, every edge is common to two adjacent triangular patches, and every node is common to at least three triangular patches as well as at least three edges.

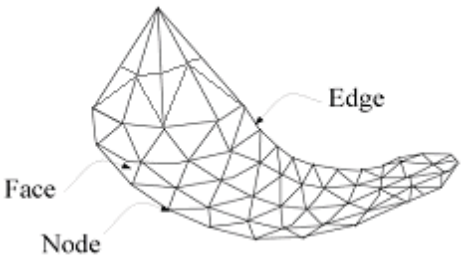

Figure 1: Triangular patch modeling of an arbitrarily shaped three-dimensional body.

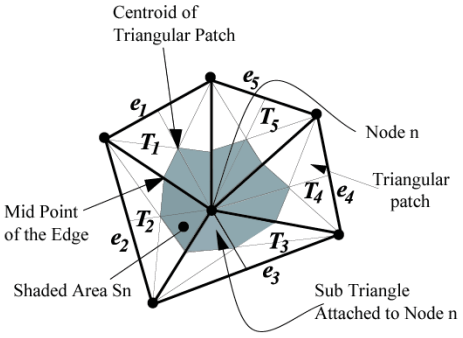

Figure 2: Node based basis function and geometric parameters associated with the node.

Consider a node n about which the basis function is defined. For illustration purposes, consider one such node as shown in Fig. 2, where there are five triangular patches attached to it. Let $T_1, T_2, ..., T_5$ are the triangular patches and $e_1, e_2, ..., e_5$ are the edges surrounding the node. The shaded region, shown in the Fig. 2. as S_n, is formed by joining the mid points of the edges, that are connected to the node n, to the centroids of adjacent triangular patches thus forming a closed boundary around the node.

Since the method of moments solution calls for the definition of expansion/basis as well as testing/weighting functions, expansion/basis functions are defined on the source node n and the testing/weighting functions are defined on the field node m.

Let there are p number of triangular patches attached to field node m and q number of triangular patches attached the source node n. By joining the node on which the basis function or weighting function is defined, to the centroid of the attached triangular patches, the shaded area on each triangular patch is divided into two sub triangles, resulting u number of sub triangles around field node m and v number of sub triangles around the source node n. In this paper, index x is used to represent the sub triangle attached to the field node and index y is used to represent the sub triangle attached to the source node.

The node based basis function is defined over the shaded area as follows.

$$f_n\left(r'\right) = \begin{cases} 1 & r' \in S_n \\ 0 & \text{Otherwise} \end{cases} \tag{21}$$

The source density function σ over the surface of the scattering object is approximated by

$$\sigma\left(r'\right) = \sum_{n=1}^{N_n} \beta_n f_n \tag{22}$$

where β_n represent the unknown coefficients to be determined and the equality sign is usually approximate. The basis functions defined over the node has all advantages as edge based basis functions [see B. Chandrasekhar and S.M. Rao (2004)].

In the numerical solution of all the three formulations, Galarkin's approach is used by defining the testing function in the same manner as it is defined for the basis function.

$$w_m = \begin{cases} 1 & r \in S_m \\ 0 & \text{Otherwise} \end{cases} \tag{23}$$

The next three sub-sections describe the numerical solution procedure for the SLF, DLF and CLF.

5.1 Single Layer Formulation (SLF)

Testing Eq. 18 with a testing function w_m , results in

$$\left\langle w_m, \frac{\sigma\left(r'\right)}{2} \right\rangle - \left\langle w_m, \int_s \sigma\left(r'\right) \frac{\partial G\left(r, r'\right)}{\partial n} ds' \right\rangle = \left\langle w_m, \frac{\partial \Phi^i}{\partial n} \right\rangle. \tag{24}$$

Using the inner product definition described in Sec. 3, Eq. 24 can be written as

$$\frac{1}{2} \int_s w_m \sigma\left(r'\right) ds - \int_s w_m \int_s \sigma\left(r'\right) \frac{\partial G\left(r, r'\right)}{\partial n} ds' ds = \int_s w_m \frac{\partial \Phi^i}{\partial n} ds. \tag{25}$$

Approximating the integration over the field node at the centroids of the attached sub triangles, and using Eq. 23, the Eq. 25 becomes

$$\frac{\sigma(r')}{2}\sum_{x=1}^{u}A_m^x-\sum_{x=1}^{u}A_m^x\int_s\sigma(r')\frac{\partial G(r_m^{cx},r')}{\partial n_m^x}ds'=\sum_{x=1}^{u}A_m^x\frac{\partial\Phi^i}{\partial n_m^x} \tag{26}$$

where A_m^x is the area of sub-triangle attached to the field node. This approximation is justified because the sub domains are sufficiently small, which is a necessary condition to obtain accurate solution using MoM. Substituting the source expansion defined in Eq. 22 into Eq. 26, results in a system of linear equations, which can be represented in the matrix form as

$$Z_{slf}X=Y \tag{27}$$

where Z_{slf} is the impedance matrix of the single layer formulation of size $N_n\times N_n$, X and Y are the column vectors of size N_n. The elements of Z_{slf}, X and Y are given below.

$$Z_{slf}^{mn}=\begin{cases}\frac{1}{2}\sum\limits_{x=1}^{u}A_m^x & \text{for } m=n \text{ and } x=y\\ -\sum\limits_{x=1}^{u}\sum\limits_{y=1}^{v}A_m^x\int_s\frac{\partial G\left(r_m^{cx},r_n^{cy}\right)}{\partial n_m^x}ds' & \text{otherwise}\end{cases} \tag{28}$$

and

$$Y^m=\sum_{x=1}^{u}A_m^x\frac{\partial\Phi^i}{\partial n_m^x} \tag{29}$$

where r_m^{cx} is the position vector to the centroid of the x^{th} sub-triangle attached to field node, r_n^{cy} is the position vector to the centroid of the y^{th} sub-triangle attached to source node and $\partial G/\partial n_m^x$ is the normal derivative of Green's function at the centroid of the x^{th} sub-triangle attached to field node.

Once the elements of the impedance matrix Z_{slf} and the forcing vector Y are determined, one may solve the linear system of equations, Eq. 27, for the unknown vector X.

Here we note that, when the frequency of the incident wave is in the close vicinity of the characteristic frequency related to Dirichlet problem, the impedance matrix Z_{slf} becomes highly ill-conditioned and the solution vector X turns out to be spurious resulting in unphysical values of source distribution σ.

5.2 Double Layer Formulation (DLF)

Testing Eq. 19 with the functions defined in Eq. 23,

$$\left\langle w_m, \int_s n \bullet n' k^2 \sigma(r') G(r,r') ds' \right\rangle + \left\langle w_m, \int_s \left(n' x \nabla' \sigma\right) \bullet (nX\nabla G)\, ds' \right\rangle = \left\langle w_m, \frac{\partial \Phi^i}{\partial n} \right\rangle. \quad (30)$$

Taking the first term for evaluation,

$$\begin{aligned} \left\langle w_m, \int_s n \bullet n' k^2 \sigma(r') G(r,r') ds' \right\rangle &= \int_s w_m \int_s n \bullet n' k^2 \sigma(r') G(r,r') ds' ds \\ &= \sum_{x=1}^{u} A_m^x n_m^x \bullet \int_s n' k^2 \sigma(r') G(r,r') ds' \end{aligned} \quad (31)$$

where n_m^x represent the unit normal vectors of the sub triangle connected to the m^{th} node. We also note that the double surface integration in Eq. 31 is converted to a single surface integral by approximating the integrand at the centroid of the sub triangle attached to m^{th} node and multiplying by the area of the sub triangle as before.

To evaluate the second term in the Eq. 30, we follow the similar procedure mentioned in [Chandrasekhar and Rao (2004)], but node based basis function are used in contrast to the edge based basis functions. The advantages of using the node based basis function are already mentioned in the earlier section.

Let us define, $J' = n' X \nabla' \sigma$ and the vector J' is again approximated by a new set of basis functions. We have,

$$J' = \sum_{f=1}^{N_f} g_f(r'). \quad (32)$$

where g_f is spread over the triangular patch and assumed to be constant. Since g_f is not an independent quantity, a relationship between β_n, f_n, and g_f may be derived as follows:

Consider the triangular patch T_f with associated non-boundary edges l_1, l_2, l_3 and nodes n_1, n_2, n_3 as shown in the Fig. 3. Then, using well-known Stoke's theorem and simple vector calculus, $J' = n' X \nabla' \sigma$ may be re-written as

$$\begin{aligned} \int_s J' ds' = \int_s n' X \nabla' \sigma ds' = \oint_{C_e} \sigma' dl' &= \frac{\beta_1 f_1 (l_2 + l_3)}{2} + \frac{\beta_2 f_2 (l_3 + l_1)}{2} + \frac{\beta_3 f_3 (l_1 + l_2)}{2} \\ &= -\frac{\beta_1 f_1 l_1 + \beta_2 f_2 l_2 + \beta_3 f_3 l_3}{2} \end{aligned} \quad (33)$$

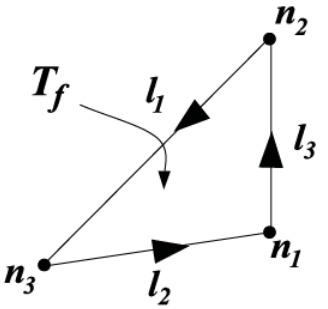

Figure 3: Triangular patch T_f and associated edges and nodes.

where C_e is the contour bounding the triangle T_f and l_i, $i = 1,2,3$ represent the edge vectors as shown in the Fig. 3. Noting that,

$$\begin{aligned} \int_s J' ds' &= \int_s g_f ds' \\ &= g_f A_{fn} \end{aligned} \tag{34}$$

where A_{fn} is the area of the triangular patch attached to the source node.

$$g_f = \frac{1}{A_{fn}} \int_s J' ds' \tag{35}$$

substituting Eq. 33 into Eq. 35, we get

$$g_f = -\frac{1}{2A_{fn}} \left(\beta_1 f_1 l_1 + \beta_2 f_2 l_2 + \beta_3 f_3 l_3\right). \tag{36}$$

This is the required relationship between β_n, f_n and g_f.
We have,

$$J' \bullet (nX\nabla G) = n \bullet \nabla G X J' = n \bullet \left(\nabla X \left[GJ'\right] - G\nabla X J'\right). \tag{37}$$

The term $G\nabla XJ'$ vanishes because the curl operation is on the unprimed variable only. Thus,

$$\int_s J' \bullet (nX\nabla G)\, ds' = n \bullet \nabla X \int_s J' G ds'. \tag{38}$$

Let $A = \int_s J' G ds'$, then the above equation can be written as

$$\int_s J' \bullet (nX\nabla G)\, ds' = n \bullet \nabla X A. \tag{39}$$

Taking the testing operation,

$$\left\langle w_m, \int_s J' \bullet (nX\nabla G)\, ds' \right\rangle = \int_s w_m (n \bullet \nabla XA)\, ds = \oint_{Cm} A \bullet dl = -\frac{l_m}{2} \bullet \left(\sum_{x=1}^{p} A\left(r_m^{cfp}\right) \right) \tag{40}$$

where p is the number of triangular patches attached to the field node and r_m^{cfp} is the position vector to the centroid of triangular patch attached to the field node. The expression for the testing operation on right hand side of the Eq. 30 is same as that of single layer formulation, i.e. Eq. 25.

Substituting Eq. 31, Eq. 40 and RHS of Eq. 26 into Eq. 30, we get

$$\sum_{x=1}^{u} A_m^x n_m^x \bullet \int_s n' k^2 \sigma(r') G(r_m^{cx}, r') ds' + \frac{l_m}{2} \bullet \left(\sum_{x=1}^{p} A\left(r_m^{cfp}, r'\right) \right) = \sum_{x=1}^{u} A_m^x \frac{\partial \Phi^i}{\partial n_m^x}. \tag{41}$$

Substituting the source expansion defined in Eq. 21 and Eq. 22, results into a system of linear equations which can be expressed in matrix form as

$$Z_{dlf} X = Y \tag{42}$$

where Z_{dlf} is the impedance matrix for double layer formulation of size $N_n \times N_n$, X and Y are column vector of size N_n.

$$Z_{dlf}^{mn} = \sum_{x=1}^{u} \sum_{y=1}^{v} k^2 A_m^x n_m^x \bullet n_n^y \int_s G(r_m^{cx}, r_n^{cy}) ds' + \frac{l_m}{2} \bullet \frac{l_n}{2A_{fn}} \left(\sum_{x=1}^{p} \sum_{y=1}^{q} \int_{sf} G\left(r_m^{cfp}, r_n^{cfq}\right) ds' \right). \tag{43}$$

Note that the integration on the first term of right hand side of the above equation is on the sub triangle attached to the source node and the integration on the second term is on the triangular patch attached to the source node.

$$Y^m = \sum_{x=1}^{u} A_m^x \frac{\partial \Phi^i\left(r_m^{cx}\right)}{\partial n_m^x} \tag{44}$$

where A_m^x is the area of the sub triangle attached to the field node, A_{fn} is the area of the triangular patch attached to the source node, r_m^{cx} is the position vector to the centroid of the x^{th} sub triangle attached to field node, r_n^{cy} is the position vector to the centroid of the y^{th} sub triangle attached to source node, r_m^{cfp} is the position vector

to the centroid of the p^{th} triangular patch attached to field node, and r_n^{cfq} is the position vector to the centroid of the q^{th} triangular patch attached to source node.

Here we again note that, as in the case of SLF, DLF also suffers from the resonance problem and the impedance matrix Z_{dlf} becomes highly ill-conditioned when the frequency of the incident wave is in the close vicinity of the characteristic frequency related to Neumann problem. The solution vector X turns out to be spurious resulting in unphysical values of source distribution σ.

5.3 Combined Layer Formulation (CLF)

Testing Eq. 20 with the functions defined in Eq. 23

$$\left\langle w_m, \frac{\sigma(r')}{2} \right\rangle - \left\langle w_m, \int_s \sigma(r') \frac{\partial G(r,r')}{\partial n} ds' \right\rangle + \alpha \left\langle w_m, \int_s n \bullet n' k^2 \sigma(r') G(r,r') ds' \right\rangle + \alpha \left\langle w_m, \int_s \left(n' x \nabla' \sigma\right) \bullet (nX \nabla G)\, ds' \right\rangle = \left\langle w_m, \frac{\partial \Phi^i}{\partial n} \right\rangle. \quad (45)$$

This can be expressed in matrix form as

$$Z_{clf}^{mn} X = Y^m \quad (46)$$

where

$$Z_{clf}^{mn} = Z_{slf}^{mn} + \alpha Z_{dlf}^{mn} \quad (47)$$

as the LHS of the above equation is a linear combination of SLF and DLF.

The impedance matrix of CLF is free from ill-conditioning at all frequencies and ensures a unique solution.

Integrals appearing in Eq. 28 and Eq. 43 may be evaluated using the techniques mentioned in [Wilton, Rao, Glisson, Schaubert, Al-Bundak, and Bulter (1984) and Hammer, Marlowe, and Stroud (1956)] for an accurate solution, as the former contains singular kernels. Here one may note that the number of integrations to carried for the case of CLF is six (three each for SLF and DLF) for each triangle in case of edge based solution [Chandrasekhar and Rao (2004b)], where as one may need twelve integrations for each triangular patch in case of Node based solution of CLF (six integrations for each SLF and DLF). However, extra time that the node based solution takes in generating the moment matrix is negligible compared to the time it saves in the solution of the linear system of equations.

For a plane wave incidence, we set

$$\Phi^i = e^{jk\hat{k} \bullet r} \quad (48)$$

where the propagation vector $\hat{k}$ is given by,

$$\hat{k} = \sin\theta_0 \cos\phi_0 a_x + \sin\theta_0 \sin\phi_0 a_y + \cos\theta_0 a_z \tag{49}$$

(θ_0, ϕ_0) define the angles of arrival of the plane wave in the conventional spherical co-ordinate system and a_x, a_y and a_z are the unit vectors along the x, y and z axes, respectively.

The normal derivative of the incident field may be written as

$$\frac{\partial \Phi^i}{\partial n} = n \bullet \nabla \Phi^i = jkn \bullet \hat{k} e^{jk\hat{k}\bullet r}. \tag{50}$$

Once the elements of the impedance matrix Z and the forcing vector Y are determined, one may solve the linear system of equations, Eqs. 27, 42 and 46, for the unknown vector X using any standard matrix inversion techniques.

6 Numerical Results

In this section, the numerical solution developed in the above sections is validated against exact solution wherever available and against the edge based solution wherever exact solutions are not available for the cases of SLF, DLF and CLF. Also the inverse condition numbers are plotted in order to demonstrate the existence of the internal resonance problem for the SLF and DLF cases and the elimination of the resonance problem for the case of CLF. The geometries considered here are simple canonical shapes like Sphere, Cube, Cylinder and a Cone. For all these cases, the body is placed at the center of the co-ordinate system and a plane wave, traveling along –Z axis is incident on the body. Here, we note that, no convergence study is carried out to ascertain the optimum number of nodes required to obtain certain degree of accuracy. The scattering cross section is defined by

$$S = 4\pi \left| \frac{\Phi^s}{\Phi^i} \right|^2 \approx \frac{1}{4\pi} \left| \sum_{n=1}^{N_n} \beta_n \left[\sum_{y=1}^{v} A_n^y n_n^y \bullet r_n^y e^{jkn_n^y \bullet r_n^y} \right] \right|^2. \tag{51}$$

In all the formulations, as a first case, a sphere of radius $1m$ and 2m are considered with triangular patch modeling. The modeling is done by dividing the θ and ϕ direction equal segments each and the complete modeling procedure is described in [Chandrasekhar and Rao (2004)]. Also the geometries with sharp corners and sharp edges such as cube, cylinder and cone are considered in order to demonstrate the capability of the node based basis functions based on method of moments solution.

6.1 Single layer formulation (SLF)

In this section, numerical results based on the SLF numerical solution procedure is presented to validate the results with the exact solution for the cases of spheres of radii 1m and 2m. Fig. 4 shows the far field scattering cross section of the sphere versus the polar angle based on the SLF for the case when the sphere of radius 1m is excited by an acoustic plane wave with $k = 1$ rad/m, traveling along –Z axis.

It is evident from the figure that, the method of moments solution based on the node based basis functions matches well with the exact solution [Bowman, Senior and Uslenghi (1969)]. In order to demonstrate the convergence of the solution, sphere is modeled with 58 nodes, 112 faces and 168 edges on the surface of the sphere; 156 nodes, 308 faces and 462 edges; as well as with 212 nodes, 420 faces and 630 edges. The results for these three cases are plotted against the exact solution for the sake of comparison.

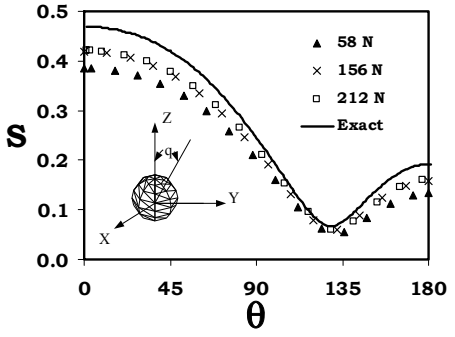

Figure 4: Scattering cross section versus polar angle for an acoustically rigid sphere of radius 1m, subjected to an axially incident plane wave of $k = 1$ rad/m, based on Single layer formulation (SLF).

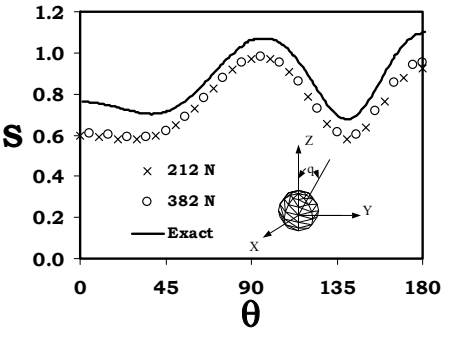

Figure 5: Scattering cross section versus polar angle for an acoustically rigid sphere of radius 2m, subjected to an axially incident plane wave of $k = 1$ rad/m, based on Single layer formulation (SLF).

As a second case, the sphere of radius 2m modeled with 212 nodes and 382 nodes are also excited by a plane wave with $k = 1$ rad/m and the scattering cross section is plotted in Fig. 5. The discrepancy between the two solutions can be attributed to insufficient number of unknowns and the fact that the surface area of the triangulated sphere is less than that of the actual sphere. The solution for SLF case can be further improved by increasing the number of unknowns.

6.2 Double layer formulation (DLF)

In this section, numerical results based on the DLF numerical solution procedure is presented to validate the results with the exact solution for the cases of spheres of radii 1m and 2m. Fig. 6 shows the results based on the DLF for the same geometries considered in the case of SLF viz 58 nodes, 156 nodes and 212 nodes. Next, the DLF numerical solution procedure is again tested and the results are shown for a plane wave incidence on a sphere of radius 2m. These results also very well match with the exact solution and the convergence of the solution is clearly evident in the Fig. 7 as the number of nodes is increased on the surface of the sphere.

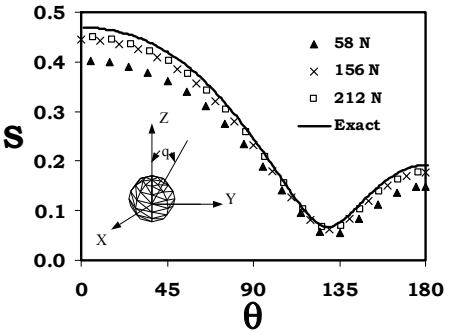

Figure 6: Scattering cross section versus polar angle for an acoustically rigid sphere of radius 1m, subjected to an axially incident plane wave of $k = 1$ rad/m, based on Double layer formulation (DLF).

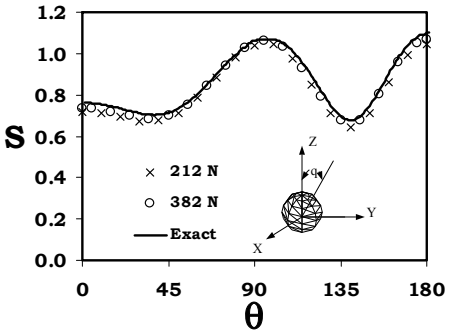

Figure 7: Scattering cross section versus polar angle for an acoustically rigid sphere of radius 2m, subjected to an axially incident plane wave of $k = 1$ rad/m, based on Double layer formulation (DLF).

The results of the DLF numerical solution procedure shown in Fig. 7 well matches with the exact solution as compared to the SLF numerical solution procedure for the case of $ka = 2$.

6.3 Combined Layer Formulation (CLF)

In this section, numerical results based on the CLF numerical solution procedure is presented to validate the results with the exact solution for the cases of spheres of radii 1m and 2m. The complex coupling parameter considered in the CLF solution is $\alpha = 0.1\,j$, though this value is not critical.

In order to demonstrate the capability of the node based SLF, DLF and CLF solution, geometries with sharp edges and sharp corners are considered in the following paragraphs.

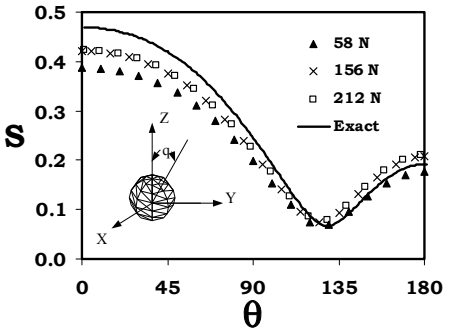

Figure 8: Scattering cross section versus polar angle for an acoustically rigid sphere of radius 1m, subjected to an axially incident plane wave of $k = 1$ rad/m, based on Combined layer formulation (CLF).

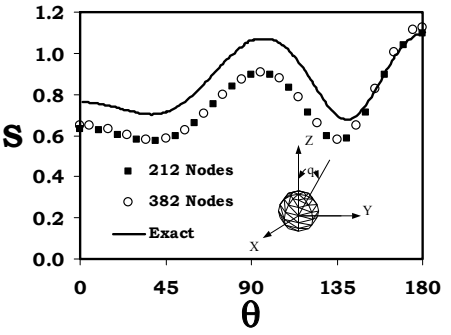

Figure 9: Scattering cross section versus polar angle for an acoustically rigid sphere of radius 2m, subjected to an axially incident plane wave of $k = 1$ rad/m, based on Combined layer formulation (CLF).

First, we consider the case of a cube with side length $l = 1m$. The case of a cube presents a challenging task of handling sharp edges and corners. To obtain a triangular patch model, each side of the cube is divided into 4 equal segments resulting in 96 square patches and 98 nodes on the cube. By joining the diagonals, we get 192 triangular patches and 288 edges. Fig. 10 shows the scattering cross section S as a function of Θ. It is evident from the figure that the constant basis functions defined over a node for SLF, DLF and CLF ($\alpha = 0.1\,j$) compare very well with that of edge based SLF (288 edges) solution. The edge based SLF solution is already validated in [Chandrasekhar and Rao (2004)]. Also, note that even though the basis functions are defined on sharp corners, the numerical results are fairly accurate. Finally, we note that the node-based conventional boundary integral methods [Schuster and Smith (1985),.Schuster (1985), Seybert, Soenarko, Rizzo, and Shippy (1985), Malbequi, Candel, Rignot (1987)] need complex calculations to obtain accurate results for this geometry.

As a next example, we consider the case of a finite cylinder of height 2.0m and 1.0m radius. The triangular patch modeling of the cylinder is obtained by dividing the length and circumference into 8 and 10 uniform segments, respectively, resulting in 80 rectangular patches. By joining the diagonals, we obtain 160 triangular patches. The cylinder is closed on both ends by circular disks which are modeled by and additional 70 triangular patches each. Thus, in total we have 152 nodes, 300 patches and 450 edges for this geometry. Fig. 11 shows the scattering cross section S as a function of Θ. For this case also, we note good comparison for SLF, DLF and CLF

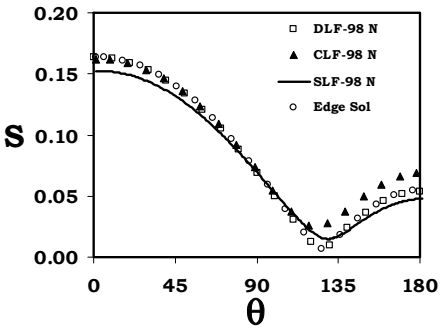

Figure 10: Scattering cross section versus polar angle for an acoustically rigid cube of length 1m, subjected to an axially incident plane wave of $k = 1$ rad/m, based on SLF, DLF and CLF.

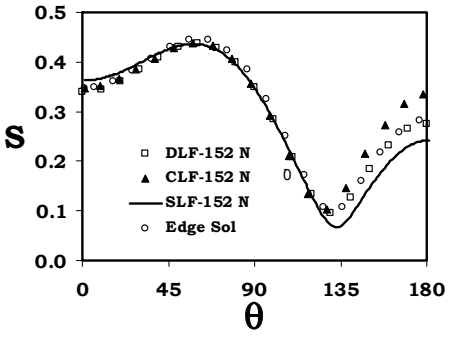

Figure 11: Scattering cross section versus polar angle for an acoustically rigid cylinder of radius 1m and height 2m, subjected to an axially incident plane wave $k = 1$ rad/m, based on SLF, DLF and CLF.

($\alpha = 0.1j$) results with the edge based SLF (450 edges) result.

Lastly, we consider a cone of 1m height and 1m radius. The cone has a sharp corner at the tip which is difficult to handle using node-based BIE methods. Using a similar discretization scheme as in the case of finite cylinder, the cone is divided into 112 nodes, 220 patches and 330 edges. Fig. 12 shows the scattering cross section S for SLF, DLF and CLF ($\alpha = 0.1j$) as a function of Θ which compares very well with the edge based SLF (330 edges) result.

6.4 Elimination of ill-conditioning problem in CLF

In this section the presence of ill-conditioning of the impedance matrices in the cases of SLF and DLF are presented along with the non-existence of the ill-conditioning for the case of CLF.

Fig. 13 shows the absolute value of logarithm of the inverse condition number of the impedance matrix of the SLF, DLF and CLF for the case of a sphere with a radius of 1m versus the wave number k. It is evident from the Fig that matrix becomes highly ill-conditioned when the frequency of the incident acoustic wave is close to or matches with the resonance frequency of cavity formed by the surface of the sphere. The matrix becomes ill-conditioned when $k = 3.19$ and $k = 2.1$ for the cases of SLF and DLF respectively. However no such phenomenon exists for the case of CLF. The corresponding theoretical values are around $k = 3.14$ and $k = 2.08$ which are the roots of the Spherical Bessel function for the Dirichlet

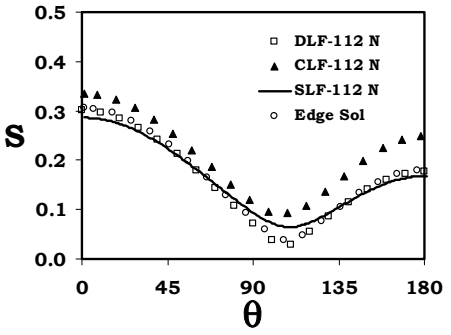

Figure 12: Scattering cross section versus polar angle for an acoustically rigid cone of radius 1m and height 1m, subjected to an axially incident plane wave $k = 1$ rad/m, based on SLF, DLF and CLF.

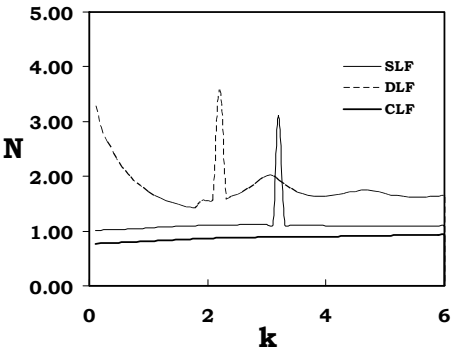

Figure 13: Condition number versus the frequency for an acoustically rigid sphere of radius 1m, subjected to an axially incident plane wave $k = 1$ rad/m, based on SLF, DLF and CLF.

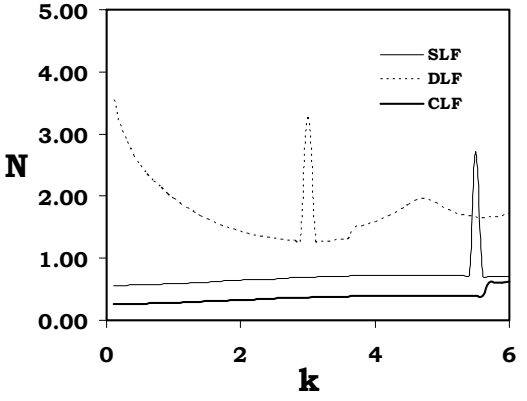

Figure 14: Condition number versus the frequency for an acoustically rigid cube of side length 1m, subjected to an axially incident plane wave $k = 1$ rad/m, based on SLF, DLF and CLF.

and Neumann problems. The difference between the numerical results and the theoretical values may be attributed to the approximation of the sphere with the triangular patch modeling.

Fig. 14 shows the absolute value of logarithm of the inverse condition number of the impedance matrix of the SLF, DLF and CLF for the case of a cube with a side length of 1m versus the wave number k. Fig shows the SLF and DLF fail around

$k = 5.4$ and $k = 3.0$ and CLF produces a conditioned matrix at all frequencies.

7 Conclusions

In this work, a novel numerical technique is presented, which implements the solution proposed by Burton and Miller in order to eliminate the resonance problem associated with the boundary integral equation formulation of the exterior acoustic scattering problem. The SLF and DLF do suffer the ill-conditioning of the resulting impedance matrix which does not exist in the case of CLF. The CLF along with SLF and DLF are solved using the method of moments solution and by defining the basis functions on the nodes. Though traditionally, DLF is difficult to solve due to the presence of hyper-singular kernel, the DLF is solved, in this work, using simple vector calculus techniques to circumvent the problems of hyper-singularity and by defining the basis functions on the nodes. Node based basis functions are defined to reduce the size of impedance matrix and hence the time required for solving the linear system of equations. Triangular patch modeling is used to approximate the surface of the scattering body. The solutions of SLF, DLF and CLF are validated with respect to the exact solutions wherever available and edge based solution wherever exact solutions are not available. However, no comparison is made in this paper on the accuracy of node based versus edge based schemes. It is clearly evident from the numerical results that, schemes based on node based basis functions converge towards the exact solutions with higher number of nodes and have advantage over the edge based basis functions from the computational complexity perspective.

References

Amini, S.; Wilton, D.T. (1986): An investigation of Boundary element methods for the exterior acoustic problem. *Computational Methods in Applied Mechanical Engineering*, vol 54, pp. 49-65.

Arefmanesh, A.; Najafi, M.; Abdi, H. (2008): Meshless Local Petrov-Galerkin Method with Unity Test Function for Non-Isothermal Fluid Flow. *CMES: Computer Modeling in Engineering and Sciences*, vol. 25, No. 1, pp. 9-22.

Bowman, J.J.; Senior, T.B.A.; Uslenghi, P.L.E. (1969): Electromagnetic and Acustic Scattering by Simple Shapes North-holland, Amsterdam.

Brakhage, H.; Werner, P. (1965); Über das Dirichletsche Aussenraumproblem fuïr die Helmholtzsche Schwingungsgleichung, *Arch. Math.*, vol 16, 325–329.

Burton, A.J.; Miller, G.F. (1971): The application of integral equation methods to the numerical solution of some exterior boundary value problems. *Proceedings of Royal Society, London*, vol A323, pp. 601-618 .

Callsen, S.; von Estorff, O.; Zaleski, O. (2004): Direct and Indirect Approach of a Desingularized Boundary Element Formulation for Acoustical Problems. *CMES: Computer Modeling in Engineering & Sciences*, Vol. 6, No. 5, pp. 421-430

Chandrasekhar, B.; Rao, S.M. (2004a): Acoustic scattering from rigid bodies of arbitrary shape –double layer formulation. *Journal of Acoustical Society of America*, vol 115, pp. 1926-1933.

Chandrasekhar, B.; Rao, S.M. (2004b): Elimination of internal resonance problem associated with acoustic scattering by three-dimensional rigid body, *Journal of Acoustical Society of America*, vol 115, pp. 2731-2737.

Chandrasekhar, B.; Rao, S.M. (2005): Acoustic Scattering from Complex Shaped Three Dimensional Structures, *CMES: Computer Modeling in Engineering & Sciences*, vol. 8, No. 2, pp. 105-118.

Chandrasekhar, B. (2005): Acoustic scattering from arbitrarily shaped three dimensional rigid bodies using method of moments solution with node based basis functions, *CMES: Computer Modeling in Engineering & Sciences*, Vol. 9, No. 3, pp. 243-254.

Chandrasekhar, B.; Rao, S.M.. (2007): Acoustic Scattering from Fluid Bodies of Arbitrary Shape. *CMES: Computer Modeling in Engineering and Sciences*, vol. 21, No. 1, pp. 67-80.

Chen, I.L.; Chen, K.H.(2006), Using the Method of Fundamental Solutions in Conjunction with the Degenerate Kernel in Cylindrical Acoustic Problems, *J. Chinese Institute of Engineers*, vol 29, No.3, 445-457.

Chen, J.T.; Chen, I.L.; Chen, K.H.(2006) A unified formulation for the spurious and fictitious frequencies in acoustics using the singular value decomposition and Fredholm alternative theorem, *J. Comp. Acoustics*, vol 14, No.2, 157-183.

Chien, C.C.; Raliyah, H.; Alturi, S.N. (1990): An effective method for solving the hyper singular integral equations in 3-D acoustics. *Journal of Acoustical Society of America*, vol 88, pp. 918-937.

Criado, R; Ortiz, J.E.; Manti c, V.; Gray, L.J.; Paris, F. (2007): Boundary Element Analysis of Three-Dimensional Exponentially Graded Isotropic Elastic Solids. *CMES: Computer Modeling in Engineering and Sciences*, vol. 22, No. 2, pp. 151.

Dang, T.D.; Bhavani V. Sankar (2008): Meshless Local Petrov-Galerkin Micromechanical Analysis of Periodic Composites Including Shear Loadings. *CMES: Computer Modeling in Engineering and Sciences*, vol. 26, No. 3, pp. 169-188.

Gao, L.; Liu, K.; Liu, Y. (2006): Applications of MLPG Method in Dynamic Fracture Problems. *CMES: Computer Modeling in Engineering and Sciences*, vol.

12, No. 3, pp. 181-196.

Hammer, P.C.; Marlowe, O.P.; Stroud, A.H. (1956): Numerical integration over simplxes and cones, *Math. Tables Aids Comp*. vol 10, pp. 130-138.

Harrington, R.F. (1968): *Field computation by Method of Moments*. MacMillan, New York.

Leis. R. (1965); Zur Dirichletschen Randwertaufgabe des Außenraumes der Schwingungsgleichung, *Math. Z.*, Vol. 90, 205–211.

Malbequi, P.; Candel, S.M. ; Rignot, E. (1987):, Boundary integral calculations of scattered fields : Application of spacecraft launcher. *Journal of Acoustical Society of America*. vol 82, pp. 1771-1781.

Maue, A.W. (1949):Zur Formulierung eines allgemeinen Beugungsproblems durch eine Integralgleichung. *Journal of Physics*, vol 126, pp. 601-618

Meyer, W. L.; Bell, W.A.; Zinn, B.T.; Stallybras, M. P. (1978): Boundary integral solutions of three dimensional acoustic radiation problems. *Journal of Sound and Vibration*, vol 59, pp. 245-262.

Mitzner, K.M. (1966): Acoustic scattering from an interface between media of greatly different density. *Journal of Mathematical Physics*. vol 7, pp. 2053-2060.

O'Neill. B. (1966): *Elementary Differential Geometry*. Academic, New York.

Owatsiriwong, A.; Phansri, B.; Park, K.H. (2008): A Cell-less BEM Formulation for 2D and 3D Elastoplastic Problems Using Particular Integrals. *CMES: Computer Modeling in Engineering and Sciences*, vol. 31, No. 1, pp. 37-60.

Panich. O. I.(1965), On the question of the solvability of the exterior boundary Problem for wave equation and Maxwell's equation (in Russian), *Usp. Mat. Nauk*, Vol. 20, 221-226.

Qian, Z.Y.; Han, Z.D.; Atluri, S.N. (2004): Directly Derived Non-Hyper-Singular Boundary Integral Equations for Acoustic Problems, and Their Solution through Petrov-Galerkin Schemes, *CMES: Computer Modeling in Engineering & Sciences*, vol. 5, No. 6, pp. 541-562

Qian, Z.Y.; Han, Z.D.; Ufimtsev, P.; Atluri, S.N. (2004): Non-Hyper-Singular Boundary Integral Equations for Acoustic Problems, Implemented by the Collocation-Based Boundary Element Method, *CMES: Computer Modeling in Engineering & Sciences*, vol. 6, No. 2, pp. 133-144.

Raju, P.K.; Rao, S. M.; Sun, S.P. (1991): Application of the method of moments to acoustic scattering from multiple infinitely long fluid filled cylinders. *Computers and Structures.* vol 39, pp. 129-134.

Rao, S.M.; Raju, P.K. (1989): Application of Method of moments to acoustic

scattering from multiple bodies of arbitrary shape. *Journal of Acoustical Society of America*. vol 86, pp. 1143-1148.

Rao, S.M.; Sridhara, B.S. (1991): Application of the method of moments to acoustic scattering from arbitrary shaped rigid bodies coated with lossless, shearless materials of arbitrary thickness. *Journal of Acoustical Society of America*. vol 90, pp. 1601-1607.

Rao, S. M.; Raju, P.K.; Sun, S.P. (1992): Application of the method of moments to acoustic scattering from fluid-filled bodies of arbitrary shape. *Communications in Applied Numerical Methods*, vol 8, pp. 117-128.

Schenck, H.A. (1968): Improved integral formulation for acoustic radiation problems. *Journal of Acoustical Society of America.* vol 44, pp. 41-58.

Schuster, G.T.; Smith, L.C. (1985): A comparison and four direct boundary integral methods. *Journal of Acoustical Society of America*. vol 77, pp. 850-864.

Schuster, G.T. (1985): A hybrid BIE + Born series modeling scheme: Generalized Born series. *Journal of Acoustical Society of America.* vol 77, pp. 865-879.

Seybert, A.F.; Soenarko, B. ; Rizzo, F.J.; Shippy, D.J. (1985): An advanced computation method for radiation and scattering acoustic waves in three dimensions. *Journal of Acoustical Society of America*. vol 77, pp. 362-368.

Sladek, J.; Sladek, V.; Wen, P. H.; Aliabadi, M.H. (2006): Meshless Local Petrov-Galerkin (MLPG) Method for Shear Deformable Shells Analysis, *CMES: Computer Modeling in Engineering & Sciences*, vol. 13, No. 2, pp. 103-118.

Sladek, J.; Sladek, V.; Solek, P.; Wen, P.H. (2008): Thermal Bending of Reissner-Mindlin Plates by the MLPG. *CMES: Computer Modeling in Engineering & Sciences*, vol. 28, No. 1, pp. 57.

Soares Jr, D.; Vinagre, M. P. (2008): Numerical Computation of Electromagnetic Fields by the Time-Domain Boundary Element Method and the Complex Variable Method. *CMES: Computer Modeling in Engineering & Sciences*, vol. 25, No. 1, pp. 1-8.

Sun, S.P.; Rao, S. M. (1992): Application of the method of moments to acoustic scattering from multiple infinitely long fluid-filled cylinders using three different formulation. *Computers and Structures*. vol 43, pp. 1147-1153.

Vavourakis, V.; Sellountos, E. J.; Polyzos, D. (2006): A comparison study on different MLPG(LBIE) formulations. *CMES: Computer Modeling in Engineering & Sciences*, vol. 13, No. 3, pp. 171-184.

Wilton, D.R.; Rao, S.M.; Glisson, A.W.; Schaubert, D.H.; Al-Bundak, O.M.; Bulter, C.M. (1984): Potential Integrals for uniform and linear source distributions on polygons and polyhedra domains. *IEEE transactions, Antennas Propagation.*

vol AP-32, pp. 276-281.

Yan, Z.Y.; Cui, F. S.; Hung, K. C. (2005): Investigation on the Normal Derivative Equation of Helmholtz Integral Equation in Acoustics. *CMES: Computer Modeling in Engineering & Sciences*, Vol. 7, No. 1, pp. 97-106.

Zai You Yan (2006): Treatment of Sharp Edges/Corners in the Acoustic Boundary Element Method under Neumann Boundary Condition. *CMES: Computer Modeling in Engineering & Sciences*, vol. 13, No. 2, pp. 81-90.

Zhang, Y.Y.; Chen, L. (2008): A Simplified Meshless Method for Dynamic Crack Growth, *CMES: Computer Modeling in Engineering & Sciences*, vol. 31, No. 3, pp. 189-200.